Catalysis Letters (2022) 152:2375–2385
https://doi.org/10.1007/s10562-021-03815-1

A Functionalized Magnetic Graphene-Based MOFs Platform as the Heterogeneous Mimic Enzyme Sensor for Glucose Detection

Ying Li[1,2] · Qian Wang[1] · Zhu Ding[1] · Dong Wan[1] · Xuetong Nie[1] · Chongli Zhong[1,2]

Received: 27 June 2021 / Accepted: 24 September 2021 / Published online: 8 October 2021

Abstract

A facile one-step route was presented to prepared NH_2-MIL-88B(Fe) and Fe_3O_4 modified reduced graphene oxide nanoparticles (NH_2-MIL-88B(Fe)@MRGO) as mimic enzymes. The as-prepared NH_2-MIL-88B(Fe)@MRGO exhibits a higher affinity for hydrogen peroxide and thus possessed a prominent peroxidase-mimic activity. Under the most favorable conditions, the hybrid nanomaterials with high catalytic velocity (2.57×10^{-7} M s^{-1}) and affinity (Km = 0.0091 mM) for substrates of H_2O_2 display a great glucose detection performance in the range of 20–800 μM with a Limit of detection (LOD) of 3.16 μM (S/N = 3).

Graphic Abstract

Favorable mimic enzymes catalysis is achieved on NH_2-MIL-88B(Fe) and Fe_3O_4 modified reduced graphene oxide nanoparticles (NH_2-MIL-88B(Fe)@MRGO) for glucose detection.

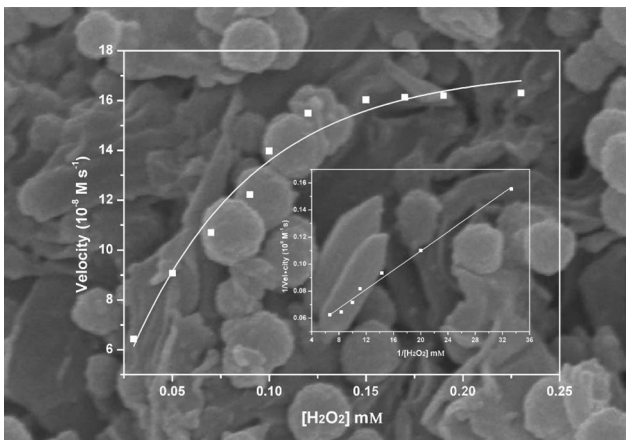

Keywords MOFs · Colorimetric method · NH_2-MIL-88B(Fe) · Peroxidase · Glucose monitoring

1 Introduction

Glucose is the energy source of human living cells and an important substance in the metabolic process, but it is easily absorbed by the blood, leading to excessive blood sugar, causing metabolic disorders, vascular disease, organ disease and other serious diseases that endanger human health [1, 2]. Therefore, it is important and necessary to establish a simple, accurate and rapid method for detecting glucose. At present, electrochemical sensing, surface-enhanced Raman

✉ Ying Li
ly@tiangong.edu.cn

[1] School of Chemical Engineering and Technology, Tiangong University, Tianjin 300387, China

[2] State Key Laboratory of Separation Membranes and Membrane Processes, Tiangong University, Tianjin 300387, China

scattering, colorimetry and fluorescence are often used to monitor glucose content [3–6]. Among them, the colorimetric method has received widespread attention because of its economy, simplicity, and its ability to be monitored through visual screening. The classic colorimetric method uses glucose oxidase (GO_x) to oxidize glucose to gluconic acid and hydrogen peroxide (H_2O_2), and monitors the glucose content through the color change process between H_2O_2 and natural peroxidase [7–10]. However, natural enzymes have limitations such as poor stability, variability, and difficulty in recycling, which are severely restricted in practical applications [11, 12].

Ever since the first artificial nanoenzyme Fe_3O_4 was reported, many peroxidase mimics such as precious metals, metal oxides, transition metal double halides have been developed [13]. Fe_3O_4 nanoparticles have peroxidase-like activity and can be used for wastewater detection through color changes [14]. In recent years, heterogeneous nanozymes have attracted widespread attention due to their advantages such as good stability, adjustable catalytic sites, and easy synthesis [15–18]. Graphene (RGO) has unique properties such as electrical conductivity, thermal stability, chemical stability, and π−π conjugated structure system, and exhibits a peroxidase activity that can catalyze the formation of active hydroxyl radicals from H_2O_2 [19, 20]. It is used as a matrix material for heterogeneous mimic enzymes to enhance the sensitivity of the colorimetric sensor in the detection process [21, 22]. For instance, anoparticles such as ZnO, Co_3O_4, CuO are often loaded on the surface of graphene for glucose sensing and detection [23]. However, the currently reported graphene-based nanozymes have the disadvantages of small specific surface area, less exposed active sites, and slightly slower colorimetric detection signals, so that their peroxidase activity needs to be further improved [24].

In recent years, the Metal organic frameworks (MOFs) as a class of porous materials has attracted much more attention due to their unique characters such as large porosity, large specific surface area and adjustable pore size [25, 26]. Due to their large specific surface area, adjustable pore size, and strong stability, they are used in adsorption, separation, biosensing and catalysis [27, 28]. The metal centers and organic ligands in the MOFs structure can be used as transport carriers for colorimetric sensing; its ordered microporous framework can provide abundant adsorption and catalytic sites [29–31], which can be used to monitor glucose in real samples [32]. Among them, MOFs with transition metal Fe^{3+} as the active center can improve the peroxidase ability of graphene and play a synergistic effect in the activation of H_2O_2 [33]. It also has similar chemical properties and excellent performance to mimic enzymes, making it an ideal candidate for enhancing the activity of graphene-based heterogeneous mimic enzymes [34]. Therefore, using MOFs (Fe) to modify graphene-based heterogeneous nanozymes is an effective method to further improve its peroxidase activity.

In this work, we proposed a facile one-step route to prepared NH_2-MIL-88B(Fe) and Fe_3O_4 modified reduced graphene oxide (RGO) mimic enzymes (NH_2-MIL-88B(Fe)@MRGO), where NH_2-MIL-88B (Fe) servers as the catalytically active component. These mimic enzymes combine the peroxidase activity of Fe_3O_4, graphene, and NH_2-MIL-88B(Fe) in one, which provide a huge active center for absorption and catalysis, leading to an enhanced peroxidase activity for detecting glucose. At the same time, a glucose detection system based on the cascade reaction of glucose oxidase (GO_x) and enhanced heterogeneous nanozyme (NH_2-MIL-88B(Fe)@MRGO) was constructed. It provides an effective strategy for the detection of H_2O_2 and glucose with high sensitivity, good stability and simple colorimetric sensing, and has great application prospects in biological analysis, disease diagnosis and pollution treatment.

2 Experimental

2.1 Chemicals and Reagents

Ferric chloride hexahydrate ($FeCl_3{\cdot}6H_2O$), Ethylene glycol (EG), sodium acetate (NaAc), acetic acid, hydrogen peroxide(30% wt%, H_2O_2) were obtained from Tianjin Sailboat Chemical Reagent Co. Ltd. Graphite, dimethyl aminoterephthalate (NH_2-BDC) were obtained from Alfa Aesar. Glucose oxidase (GO_x, 200 Umg^{-1}) was purchased from Sigma-Aldrich and stored in the refrigerator at − 20 °C. 3,3′,5,5′-Tetramethylbenzidine (TMB), glucose, fructose, maltose, lactose were purchased from Aladdin. All the reagents above were of analytical reagent grade and used without further purification. Deionized water was used throughout the experiment.

2.2 Preparation of GO and GO-COOH

Graphene oxide (GO) was prepared from purified natural graphite by a modified Hummers method [35]. GO-COOH was synthesized as follows: 5 g NaOH were dissolved in 100 mL of deionized water. After the solid was cooled down to room temperature, 100 mg GO and 5 g sodium chloroacetate was added into the above solution and sonicated for 30 min. Finally, the products were thoroughly washed several times with ethanol and water until the pH of the product reached about 7.0, and dried in vacuum overnight.

2.3 Preparation of MRGO and MRGO-COOH

Magnetic oxidized graphene (MRGO) was synthesized by a hydrothermal method as precious describe [36]. Briefly,

100 mg GO was dispersed into a solution consists of 60 mL EG. The mixture was ultrasonically treated for 10 min before 1.620 g $FeCl_3$, 0.353 g sodium citrate, and 4.320 g NaAc were introduced and stirred for 1 h at room temperature. After that, the mixture was transferred to 30 mL Teflon-lined stainless autoclaves and heated for 12 h at 200 °C under autogenous pressure. After the autoclave was cooled down to room temperature, the precipitate was filtered, washed with distilled water, and ethanol for several times, and dried in a vacuum oven at 60 °C for 12 h.

100 mg MRGO was dissolved in deionized water firstly and sonicated for 30 min, 5.00 g NaOH and 5.00 g $NaClO_3$ were added into the above solution. The mixture was sonicated for 1 h. The as-prepared product, carboxylated magnetic oxidized graphene (MRGO-COOH), was washed by ethanol until the pH of the product reached about 7.0. Afterward, the product was dried in a vacuum oven at 60 °C for 12 h.

2.4 Preparation of NH_2-MIL-88B(Fe)

The synthesis of NH_2-MIL-88B(Fe) NPs was based on the previous report [37]. Briefly, 0.675 g $FeCl_3{\cdot}6H_2O$ and 0.225 g NH_2-BDC were dissolved in 15 mL DMF and sonicated until a homogeneous solution was observed. The mixed solution was ultrasound and then transferred to a Teflon-lined stainless-steel autoclave and was heated at 110 °C for 30 h. After cooling to room temperature, the final product was centrifugated, purified by a double treatment in ethanol and DMF, and dried in a vacuum at 60 °C.

2.5 Preparation of NH_2-MIL-88B(Fe)@GO and NH_2-MIL-88B(Fe)@MRGO

The process of synthesizing NH_2-MIL-88B(Fe)@GO and NH_2-MIL-88B(Fe)@MRGO was as follows: 0.675 g $FeCl_3{\cdot}6H_2O$ and 0.225 g NH_2-BDC were dissolved in 15 mL DMF and sonicated for 30 min. 100 mg GO-COOH or MRGO-COOH was added into the above solution and sonicated until a homogeneous solution was observed. The mixed solution was then transferred to a Teflon-lined stainless-steel autoclave and was heated at 110 °C for 24 h. After cooling to room temperature, the final product was centrifugated, purified by a double treatment in ethanol and DMF, and dried in a vacuum at 60 °C.

2.6 Kinetics Measurements

The peroxidase-like activity of NH_2-MIL-88B(Fe)@MRGO was investigated by monitoring the absorbance of TMB at 652 nm with UV–vis spectrophotometer. The stock solution of TMB(1 mM) was prepared with anhydrous ethanol using 0.4 mg mL^{-1} NH_2-MIL-88B(Fe)@MRGO in 1 mL of acetate buffer (0.2 M, pH = 4) in the presence of 50 μL of TMB (1 mM) and H_2O_2 (20–800 μM) as the substrates with a total reaction volume of 1.15 mL at room temperature. The Michaelis–Menten constant was calculated by using Lineweaver–Burk plots of the double reciprocal of the Michaelis–Menten equation: $V = V_{max} \times [S]/(K_m + [S])$. where V is the initial velocity, V_{max} represents the maximal reaction velocity, [S] corresponds to the substrate concentration, and K_m is the Michaelis–Menten constant.

2.7 Detection of H_2O_2 and Glucose

A series of H_2O_2 solution with the concentration range from 20 to 800 μM were freshly prepared. The colorimetric assay was constructed as follows: 50 μL of NH_2-MIL-88B(Fe)@MRGO particles (0.4 mg·mL^{-1}) were mixed with 1 mL of acetate buffer (0.2 M, pH = 4), 50 μL of TMB(1 mM) stock solution and 50 μL of H_2O_2 (20–800 μM) solution. After incubation at 45 °C for 20 min, NH_2-MIL-88B(Fe)@MRGO particles were magnetically removed from the reaction system. The supernatant was measured by a UV spectrophotometer and the maximal absorbance of oxidized TMB was recorded at 652 nm.

For the determination of Glucose, 20 μL GO_x (20 mg mL^{-1}) was added into a phosphate buffer solution (PBS, 0.01 M, pH = 6.0) containing different amounts of glucose and incubated at 37 °C for 20 min. After that, the above solution was added into a 200 μL of acetate buffer (0.2 M, pH 6.0) containing 50 μL of TMB (1 mM) and 300 μL NH_2-MIL-88B(Fe)@MRGO (0.4 mg mL^{-1}) in a total volume of 0.875 mL. The resulted solution was incubated at 37 °C for 15 min and the supernatant was subjected to absorbance spectroscopy measurement.

3 Results and Discussion

3.1 Characterization of NH_2-MIL-88B(Fe)@MRGO and Its Analogues

The morphology of the as-prepared samples, NH_2-MIL-88B(Fe), calcined NH_2-MIL-88B(Fe), NH_2-MIL-88B(Fe)@GO, NH_2-MIL-88B(Fe)@MRGO, was firstly investigated by TEM characterization. Figure 1a shows that NH_2-MIL-88B(Fe) has a hexagonal biconical prism structure with a length of ~ 700 nm. It can be seen from Fig. 1b that there are nanoparticles on the surface of the calcined NH_2-MIL-88B(Fe), but the basic morphological structure of the NH_2-MIL-88B(Fe) derivative is maintained. We see that NH_2-MIL-88B(Fe) is uniformly distributed on the surface of GO, and the morphology and structure of the two themselves have not changed (inserted TEM image in Fig. 1c), indicating the success of the binary material

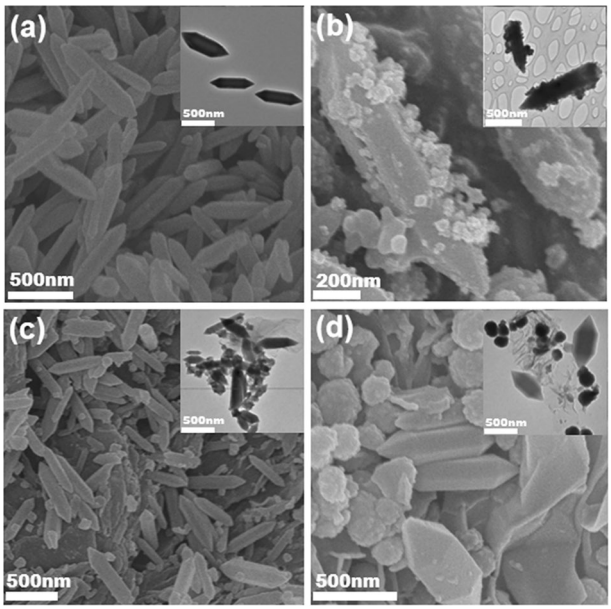

Fig. 1 Morphology of **a** NH_2-MIL-88B(Fe), **b** calcined NH_2-MIL-88B(Fe), **c** NH_2-MIL-88B(Fe)@GO, **d** NH_2-MIL-88B(Fe)@MRGO

of (002), (101), (102), (103), (200), (201) planes of metallic NH_2-MIL-88B(Fe), respectively (see curve a). This indicates that NH_2-MIL-88B(Fe) is successfully synthesized in this study. Once NH_2-MIL-88B(Fe) was calcined at 400 ºC for 10 min, the XRD patterns of calcined samples was in agreement with that of Fe_3O_4 (see curve b), which demonstrate that NH_2-MIL-88B(Fe) has transformed into Fe_3O_4. Notably, the diffraction peaks of NH_2-MIL-88B(Fe) and GO were both observed for NH_2-MIL-88B(Fe)@GO and NH_2-MIL-88B(Fe)@MRGO, indicating NH_2-MIL-88B(Fe) were deposited on the layers of GO and MRGO respectively. In particular, in NH_2-MIL-88B(Fe)@MRGO the diffraction peaks of Fe_3O_4 are seen, indicating Fe_3O_4 microspheres are successfully introduced combing with the SEM observation of NH_2-MIL-88B(Fe)@MRGO (Fig. 1d).

Fourier-transform infrared (FTIR) was used to investigate the functional groups on the surface of NH_2-MIL-88B(Fe)@MRGO. As shown in Fig. 2b, the characteristic peaks of the as-prepared NH_2-MIL-88B(Fe) are almost identical to C=C at around 1584 cm (see curve b) 1. The peaks at 1372 cm^{-1} are attributed to the symmetric stretching of C–N. These characteristic peaks also appeared in FTIR spectrum of NH_2-MIL-88B(Fe)@RGO. This observa-

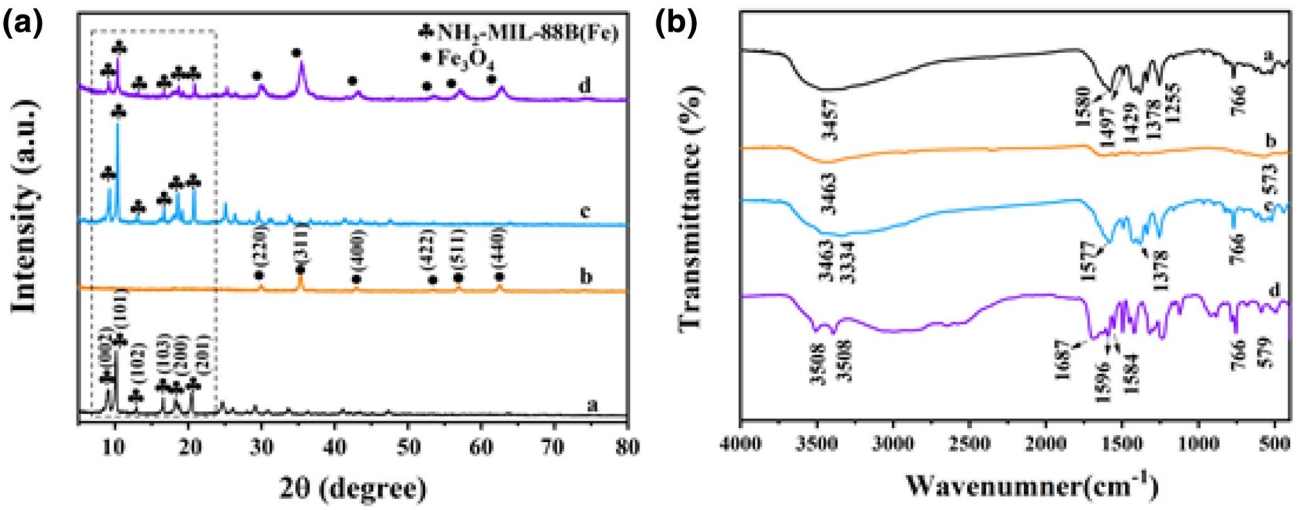

Fig. 2 The XRD pattern **a** FTIR spectra **b** of NH_2-MIL-88B(Fe) (curve a), calcined NH_2-MIL-88B(Fe) (curve b), NH_2-MIL-88B(Fe)@GO (curve c), NH_2-MIL-88B(Fe)@MRGO (curve d)

NH_2-MIL-88B(Fe)@GO preparation. After introduction of Fe_3O_4, we find that Fe_3O_4 and NH_2-MIL-88B(Fe) are adhered well to the surface of wrinkled RGO.

The crystallographic structures of the samples were further characterized using XRD technique. As shown in Fig. 2a. All the peaks of the as-prepared sample coincide with the standard NH_2-MIL-88B(Fe) [37]. Definitely, the diffraction peaks at 9.03°, 10.11° and 12.94°,16.52°,18.28°,20.61° are assigned to the diffraction

tion indicates MRGO was successfully composited with NH_2-MIL-88B(Fe). Besides, the peak at 590 cm^{-1} belonged to the Fe–O symmetric stretching of Fe_3O_4 is seen. This observation confirms the successful combination of Fe_3O_4 with NH_2-MIL-88B(Fe)@RGO.

The nitrogen adsorption–desorption isotherms and pore size distribution were conducted for calcined NH_2-MIL-88B(Fe), NH_2-MIL-88B(Fe)@

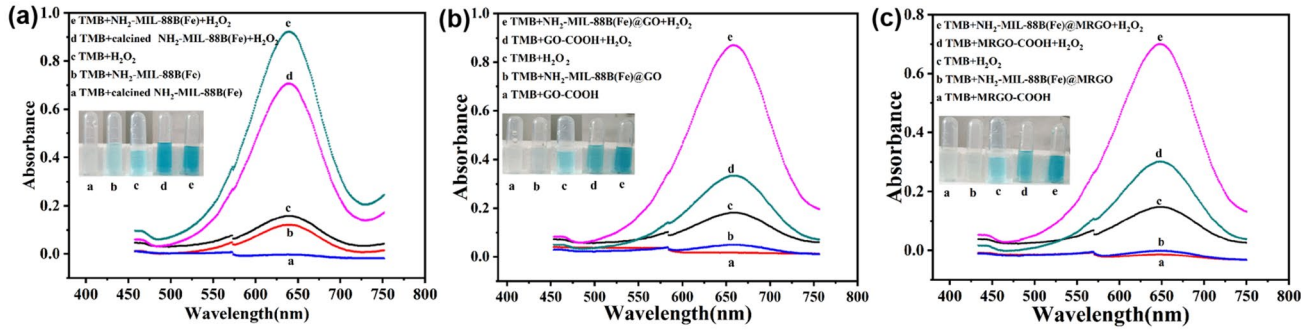

Fig. 3 Absorption spectra and digital photos of different colorimetric reaction systems: NH_2-MIL-88B(Fe) and calcined NH_2-MIL-88B(Fe) (**a**), NH_2-MIL-88B(Fe)@GO (**b**), NH_2-MIL-88B(Fe)@MRGO (**c**)

GO and NH_2-MIL-88B(Fe)@MRGO (Fig. S1). The Brunauer–Emmett–Teller(BET) surface areas of calcined NH_2-MIL-88B(Fe), NH_2-MIL-88B(Fe)@GO and NH_2-MIL-88B(Fe)@MRGO were 52.72 m^2g^{-1}, 58.97 m^2g^{-1}, 113.07 m^2g^{-1}, respectively. Thus, the introduction of graphene and Fe_3O_4 results in the increase in the specific surface. Additionally, they all exhibited a type-IV isotherm being representative of mesoporous structure which was prerequisite for an efficient sensing device.

3.2 Peroxidase Mimic Activity

To investigate the catalytic activity of various mimic enzymes, the typical peroxidase substrate 3,3′,5,5′-tetramethylbenzidine (TMB) was chosen as the chromogenic substrate in the presence of H_2O_2. The catalytic activities of four mimic enzymes (NH_2-MIL-88B(Fe) and its analogues) were monitored using UV–vis absorption spectroscopy to quantitatively analyze the amount of decomposed H_2O_2 (Fig. 3). In the absence of mimic enzymes or H_2O_2, no oxidation reaction of TMB occurred as no change in solution color was observed, indicating that both mimic enzymes and H_2O_2 were indispensable for the catalytic reaction [38–40]. Once the as-prepared mimic enzymes and H_2O_2 were introduced, the strong characteristic absorption peak at 652 nm was observed. Meanwhile, a blue color was seen (see insert in Fig. 3), a characteristic chromatogenic reaction for the formation of charge-transfer complexes which originates from the one-electron oxidation of TMB (oxTMB) [41, 42]. These results indicated that these as-prepared mimic enzymes can efficiently catalyze the oxidation of TMB by H_2O_2 and have a strong intense colorimetric response to H_2O_2. Consequently, well-performed mimic enzymes based on NH_2-MIL-88B(Fe) are successfully constructed as the sensitive colorimetric sensing platform. Of note, the adsorption peaks for NH_2-MIL-88B(Fe) and calcined NH_2-MIL-88B(Fe) mimicking enzymes is slightly shifted to the left, compared with the NH_2-MIL-88B(Fe)@GO and NH_2-MIL-88B(Fe)@MRGO. The reason is that the composite mimic enzymes have a π-π conjugated structure system originating from GO and MRGO, which will slightly reduce the ultraviolet absorption energy of the reaction system. Eventually, a slight increase in λ_{max} and a slight red shift of the absorption peak to the right are observed for NH_2-MIL-88B(Fe) and calcined NH2-MIL-88B(Fe).

3.3 Optimization of Experimental Conditions

The catalytic properties of mimic enzyme are affected by some environmental factors. To obtain the maximum catalytic ability of NH_2-MIL-88B(Fe)@MRGO, the experimental conditions were optimized, including temperatures were changed (30–60 °C), reaction time (5–35 min), H_2O_2 concentration (0–25 μM) and pH (0–12) were varied to optimize the experiment condition (Fig. S2). The optimum conditions for the detection should be pH of 4, time of 20 min, temperature of 45 °C and H_2O_2 concentration of 10 μM.

3.4 Biomorphic Detection of H_2O_2

On the basis of the peroxidase-like property of NH_2-MIL-88B(Fe) and its analogues, we used a simple colorimetric method to detect H_2O_2 as described above. Figure 4 shows the change in the absorbance intensity at 652 nm with the concentration of H_2O_2. The absorbance at 652 nm is gradually enhanced with the increasing concentration of H_2O_2 and finally reached equilibrium steady state. UV absorption of NH_2-MIL-88B(Fe)@MRGO reached a plateau at the H_2O_2 concentration of 150 μM outperforming of NH_2-MIL-88B(Fe) (300 μM), calcined NH_2-MIL-88B(Fe) (400 μM) and NH_2-MIL-88B(Fe)@GO(175 μM). More importantly, the gradual increase of absorbance shown a good linearity with below the saturation concentration of H_2O_2. Such a good linear relationship can be used as the

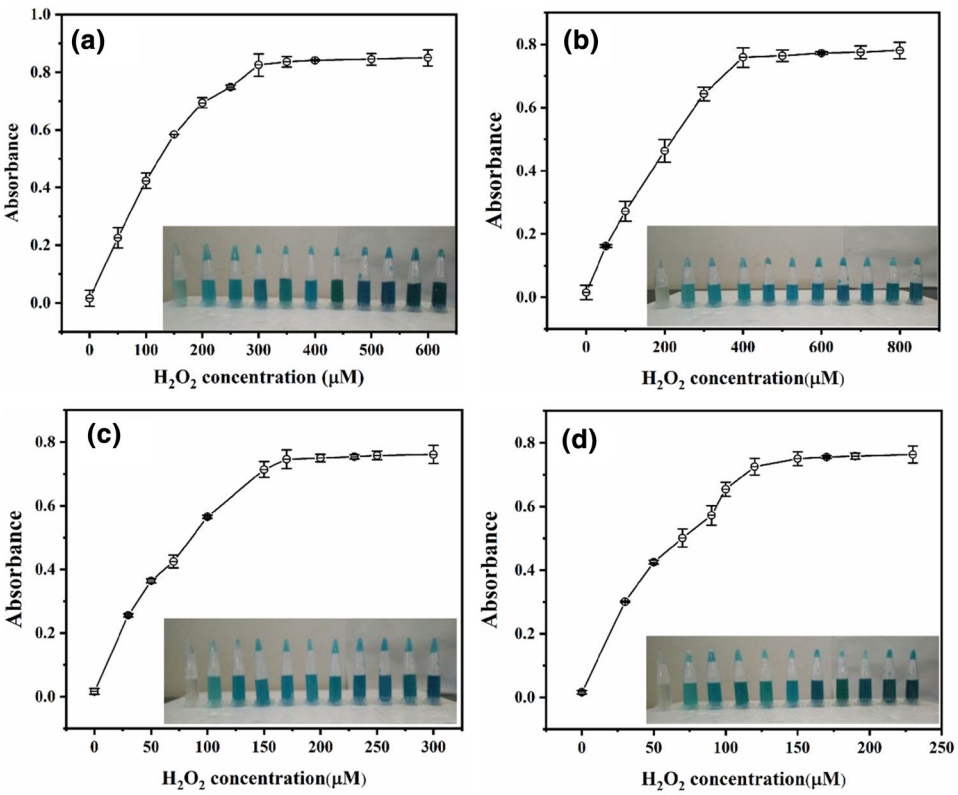

Fig. 4 Absorbance change with increasing concentration of H_2O_2: NH_2-MIL-88B(Fe) (**a**) and calcined NH_2-MIL-88B(Fe) (**b**), NH_2-MIL-88B(Fe)@GO (**c**), NH_2-MIL-88B(Fe)@MRGO (**d**) (Inset: The inset photograph is the color changes corresponding to the different reaction systems at varying H_2O_2 concentration)

standard curve for quantifying H_2O_2 in aqueous solution (Fig. S3).

3.5 Steady-State Kinetic Assay of NH_2-MIL-88B(Fe)@MRGO

To evaluate mimic enzyme catalysis of NH_2-MIL-88B(Fe)@MRGO, we first carried out the steady-state kinetic assays of GO and MRGO. It is found that the catalytic reaction rates of GO and MRGO increase at the same time as the concentration of H_2O_2 increases (Fig. S4). The Lineweaver–Burk diagram follows the typical Michaelis–Menten mechanism, showing a good linear relationship. K_m is an indicator of the affinity of the enzyme and the substrate. The K_m value is inversely proportional to the affinity between the catalyst and the substrate. The V_{max} and K_m values shown in Table S1 indicate that graphene oxide and MRGO, as the substrate materials for the heterogeneous mimetic enzyme prepared in this paper, both exhibit a certain catalytic affinity for H_2O_2 and may promote NH_2-MIL-88B(Fe)@GO and NH_2-MIL-88B(Fe)@MRGO mimic enzyme activity.

Further, steady-state kinetic constants were investigated to elucidate further the peroxidase activity of four mimic enzymes. These constants were determined by varying the concentrations of H_2O_2 while keeping the concentration of TMB at a fixed concentration in detection system. Resultantly, the Michaelis–Menten constant (K_m) and maximum initial rate (V_{max}) are determined using a Lineweaver–Burk plot. As displayed in Fig. 5, as the concentration of TMB and H_2O_2 increased, the reaction rate of mimic enzyme catalysis increased simultaneously. As depicted in the inserts, The Lineweaver–Burk plots followed a typical Michaelis–Menten mechanism [43, 44]. It is known that K_m is an indicator of enzyme affinity to substrates. the Km value is inversely proportional to the affinity between catalyst and substrates. Obviously, NH_2-MIL-88B(Fe), calcined NH_2-MIL-88B(Fe), NH_2-MIL-88B(Fe)@GO, NH_2-MIL-88B(Fe)@MRGO all exhibited favorable catalytic affinity toward H_2O_2. As seen in Table 1, the V_{max} and K_m values of four mimic enzymes were listed. These as-prepared mimic enzymes well-perform the samples as reported previously in mimic enzyme catalysis. Moreover, the values of K_m and V_{max} for the NH_2-MIL-88B(Fe)@MRGO with H_2O_2 were calculated to be 0.0091 mM and 2.57×10^{-7} M s^{-1}. By comparing the apparent kinetic parameters of other mimic enzyme, the values of K_m NH_2-MIL-88B(Fe)@MRGO was the lowest, and the V_{max} was the highest [45, 46], indicating that NH_2-MIL-88B(Fe)@MRGO nanoparticles has the largest affinity for substrates.

3.6 Glucose Detection Using NH_2-MIL-88B(Fe)@MRGO

It is well-known that glucose can be oxidized in the oxidation reaction by glucose oxidase (GO_x) to gluconolactone and H_2O_2. NH_2-MIL-88B(Fe)@MRGO and H_2O_2 simulate

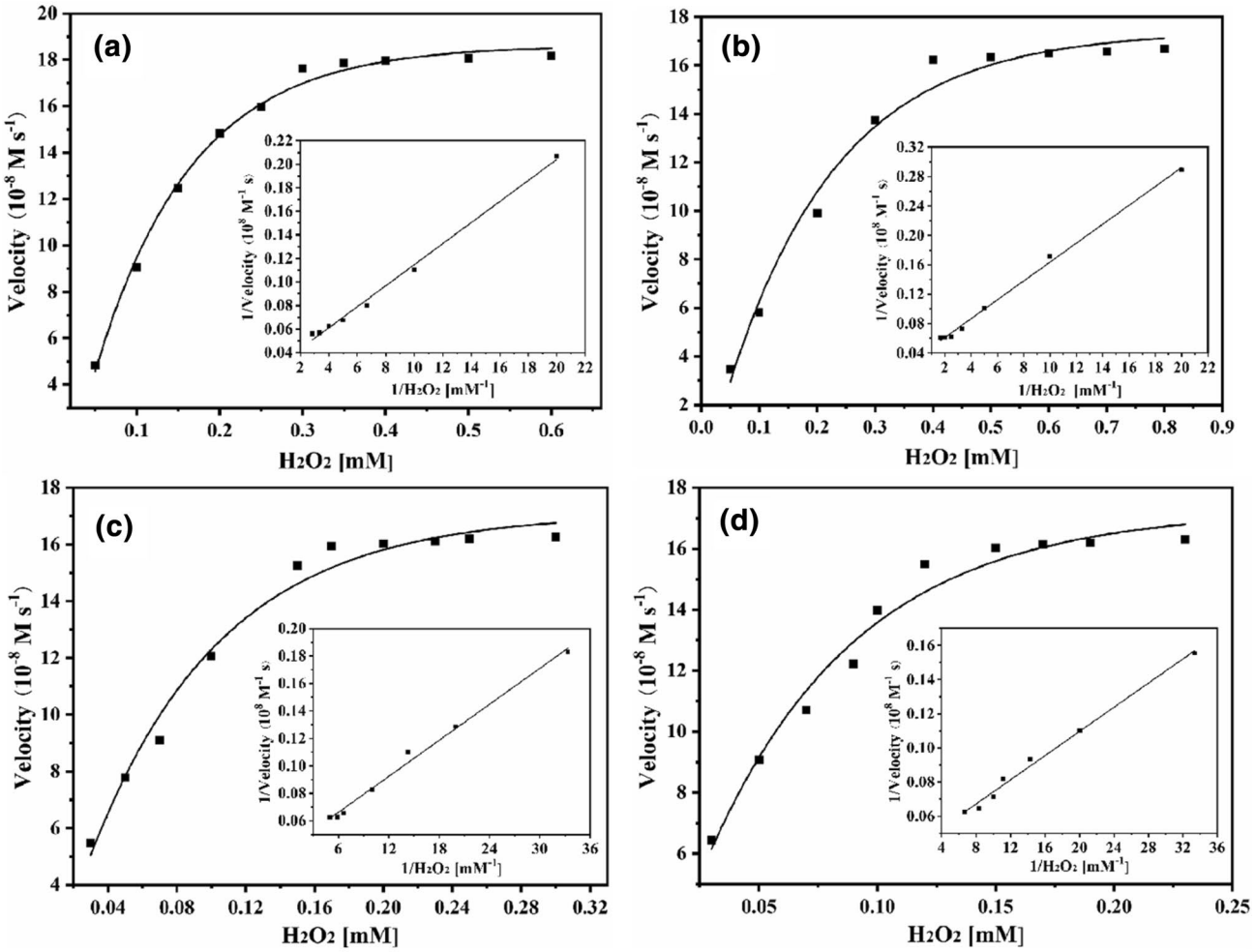

Fig. 5 Steady-state kinetic assay and catalytic mechanism of NH_2-MIL-88B(Fe) (**a**) and calcined NH_2-MIL-88B(Fe) (**b**), NH_2-MIL-88B(Fe)@GO (**c**), NH_2-MIL-88B(Fe)@MRGO (**d**). The velocity (v) of the reaction was measured using 0.4 mg mL^{-1} four kind of nanoparticles in 1 mL of HAc-NaAc buffer solution (0.2 M, pH = 4) at 45 °C, respectively. The concentration of TMB was 1 mM for four mimic enzymes and the H_2O_2 concentration varied. The inset image is the Linear correlation between concentration of $1/H_2O_2$ concentration and 1/velocity

Table 1 Comparison of Michaelis–Menten constants (K_m) and maximum reaction rates (V_{max})

Catalyst	Substrate	K_m (mM)	V_{max} (Ms^{-1})	References
NH_2-MIL-88B(Fe)	H_2O_2	0.0355	3.97×10^{-7}	This work
Calcined NH_2-MIL-88B(Fe)	H_2O_2	0.0365	2.84×10^{-7}	This work
NH_2-MIL-88B(Fe)@GO	H_2O_2	0.0109	2.51×10^{-7}	This work
NH_2-MIL-88B(Fe)@MRGO	H_2O_2	0.0091	2.57×10^{-7}	This work
Fe-MIL-88NH_2	H_2O_2	2.06	7.04×10^{-8}	[46]
$NiFe_2O_4$ MNPs	H_2O_2	2.6	14.11×10^{-8}	[47]
Fe_3O_4/N-GQDS	H_2O_2	1.02	2.76×10^{-8}	[48]
MIL-53(Fe)	H_2O_2	0.04	1.86×10^{-8}	[49]
Hemin@MIL-101(Al)-NH_2	H_2O_2	10.9	8.98×10^{-8}	[50]

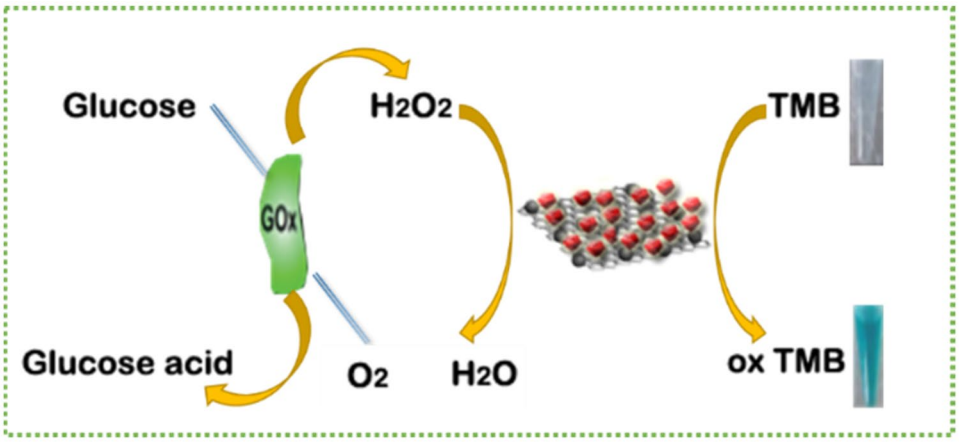

Fig. 6 Illustration of the glucose detection via the decomposition of H_2O_2 catalyzed by NH_2-MIL-88B(Fe)@MRGO

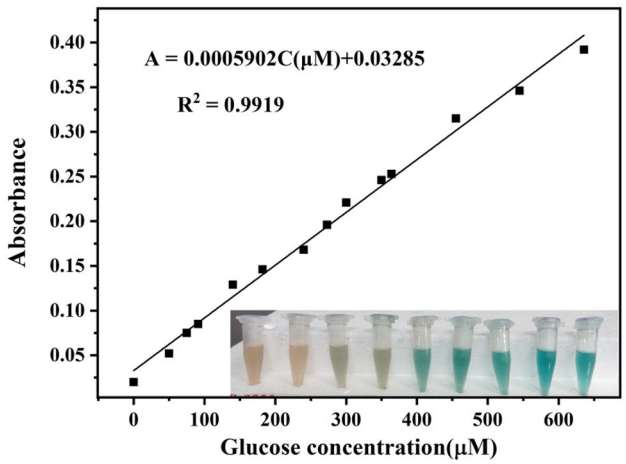

Fig. 7 Linear response of the detection system to glucose using NH_2-MIL-88B(Fe)@MRGO (Inset: The inset photograph is the color changes corresponding to the different reaction systems at varying glucose concentration)

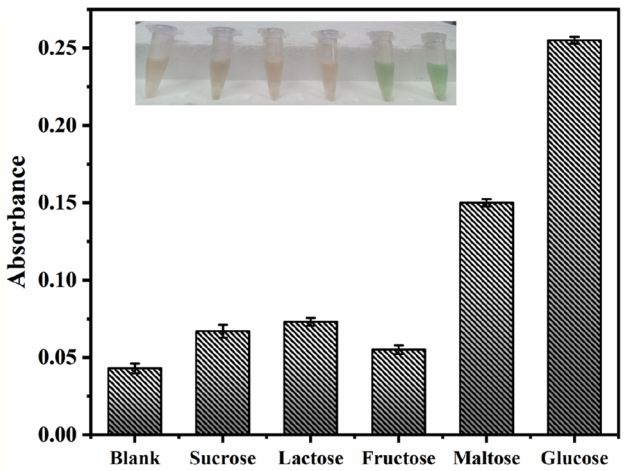

Fig. 8 Selectivity analysis for glucose detection using GO_x and NH_2-MIL-88B(Fe)@MRGO catalyst by monitoring the relative absorbance (inset: the color change corresponding to different sample)

the interaction of peroxidase and TMB, which is achieved by the color reaction of TMB analysis (Fig. 6). This property has been developed for the fabrication of glucose sensors with high sensitivity and selectivity [51, 52].

According to the above mechanism, we built a sensitive colorimetric sensing platform for glucose detection. As presented in Fig. 7, the absorption spectra of oxide TMB increased as the concentration of glucose increased, and the absorbance was linearly correlated to glucose concentration from 20 to 800 μM. The linear regression equation is A = 0.0005902 C (μM) + 0.03285 with a reliable correlation coefficient. As calculated from the linear calibration plots, the detection limit of the constructed colorimetric sensing platform was 3.16 μM, which is comparable or even superior to those achieved by using other colorimetric methods. Therefore, the established colorimetric sensing platform possesses prominent performance with high sensitivity and simplicity.

In addition, excellent peroxidase analog materials should have good peroxidase activity, but also have high selectivity to glucose. To evaluate the selectivity of the colorimetric method for glucose, control experiments were performed in the presence of glucose analog substances including 5 mM fructose, 5 mM maltose, 5 mM lactose and 5 mM sucrose (Fig. 8). The absorption intensity of glucose was much higher than its analogues; no obvious blue color is observed for other compounds except maltose. The above observations indicate that our sensing system exhibits excellent selectivity for glucose.

A good peroxidase analogue not only has a good peroxidase activity, but also have a higher practicality for glucose. In order to evaluate the ability of NH_2-MIL-88B(Fe)@MRGO to detect glucose in beverages, it was carried out in the presence of glucose mimics

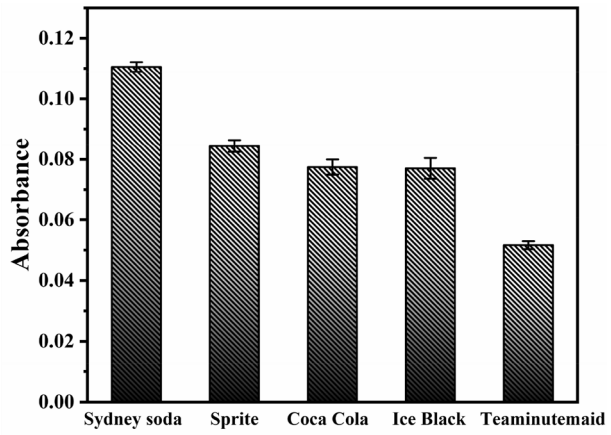

Fig. 9 Analysis for glucose detection in real samples using GO_x and NH_2-MIL-88B(Fe)@MRGO catalyst by monitoring the relative absorbance

of 5 mM Sydney soda, 5 mM Sprite, 5 mM Coca cola, 5 mM Ice Black and 5 mM Teaminutemaid (Fig. 9). It can be seen from the figure that NH_2-MIL-88B(Fe)@MRGO has a certain response to glucose in five kinds of beverages, indicating that the peroxidase analogues synthesized in this study can be used in actual samples.

4 Conclusion

In summary, MOFs-based mimic enzymes were successfully synthesized by a simple and effective method. These mimic enzymes were functionalized with the peroxidase-mimic activity of Fe_3O_4, graphene, and NH_2-MIL-88B(Fe), due to a huge active center for absorption and catalysis. NH_2-MIL-88B(Fe)@MRGO was used for biomimetic detection of glucose. This mimic enzyme shows a high catalytic velocity (2.57×10^{-7} M s^{-1}) and affinity ($K_m = 0.0091$ mM) for substrates of H_2O_2. A limit of detection (LOD) for glucose reaches 3.16 µM. Such MOFs-based offers a unique platform for the development of highly stable and efficient mimic enzymes in catalysis, biosensing and medical diagnosis.

Supplementary Information The online version contains supplementary material available at https://doi.org/10.1007/s10562-021-03815-1.

Acknowledgements This work was supported by the National Natural Science Foundation of China (220782462, 1106101, 21475095) and the Tianjin Natural Science Foundation Project (13JCQNJC06300) and China Postdoctoral Fund Project (2013M540281).

References

1. Xu WQ, Jiao L, Yan HY, Chen LJ, Gu WL, Du D, Lin YH, Zhu CZ (2019) Glucose oxidase-integrated metal-organic dramework hybrids as biomimetic cascade nanozymes for ultrasensitive glucose biosensing. ACS Appl Mater Interfaces 11:22096–22101
2. Bao YW, Hua XW, Ran HH, Zeng J, Wu FG (2019) Metal-doped carbon nanoparticles with intrinsic peroxidase-like activity for colorimetric detection of H_2O_2 and glucose. J Mater Chem B 7:296–304
3. Kim K, Kim H, Jo EJ, Jang H, Park J, Jung GY, Kim MG (2021) Reactant/polymer hybrid films on p-n junction photodetectors for self-powered, non-invasive glucose biosensors. Biosen Bioelectron 175:112855
4. Shen JW, Li YB, Gu HS, Xia F, Zuo XL (2014) Recent development of sandwich assay based on the nanobiotechnologies for proteins, nucleic acids, small molecules, and ions. Chem Rev 114:7631–7677
5. Mao GB, Cai Q, Wang FB, Luo CL, Ji XH, He ZK (2017) One-step synthesis of rox-DNA functionalized CdZnTeS quantum dots for the visual detection of hydrogen peroxide and blood glucose. Anal Chem 89:11628
6. Dong L, Li RY, Wang LQ, Lan XF, Sun HT, Zhao Y, Wang LG (2021) Green synthesis of platinum nanoclusters using lentinan for sensitively colorimetric detection of lucose. Int J Biol Macromol 172:289–298
7. Liu M, Zhao HM, Chen S, Yu HT, Quan X (2012) Interface engineering catalytic graphene for smart colorimetric biosensing. ACS Nano 6:3142–3151
8. Ge SG, Liu WY, Liu HY, Liu F, Yu JH, Yan M, Huang JD (2015) Colorimetric detection of the flux of hydrogen peroxide released from living cells based on the high peroxidase-like catalytic. Biosen Bioelectron 71:456–462
9. Lu N, Zhang M, Ding L, Zheng J, Zeng CX, Wen YL, Liu G, Aldalbahi A, Shi JY, Song SP, Zuo XL, Wang LH (2017) Yolk-shell nanostructured Fe_3O_4@C magnetic nanoparticles with enhanced peroxidase-like activity for label-free colorimetric detection of H_2O_2 and glucose. Nanoscale 9:4508–4515
10. Liu WD, Guo JN, Chen CX, Ni PJ, Jiang YY, Zhang CH, Wang B, Lu YZ (2021) Ultrathin PdCu alloy nanosheet-assembled 3D nanoflowers with high peroxidase-like activity toward colorimetric glucose detection. Microchim Acta 188:114
11. Wolfenden R, Snider MJ (2001) The depth of chemical time and the power of enzymes as catalysts. Acc Chem Res 34:938–945
12. Wang JN, Bao MY, Wei TX, Wang ZY, Dai ZH (2020) Bimetallic etaleorganic framework for enzyme immobilization by biomimetic mineralization: constructing a mimic nzyme and simultaneously immobilizing natural enzymes. Anal Chim Acta 1098:148–154
13. Wei H, Wang EK (2008) Fe_3O_4 magnetic nanoparticles as peroxidase mimetics and their applications in H_2O_2 and glucose detection. Anal Chem 80:2250–2254
14. Gao L, Zhuang J, Nie L, Zhuang JB, Zhuang Y, Gu N, Wang T, Feng J, Yang DL, Perrett S, Yan XY (2009) Intrinsic peroxidase-like activity of ferromagnetic nanoparticles and its application in immunoassay and environment treatment. Nat Nanotech 2:577–583
15. Lin YH, Ren JS, Qu XG (2014) Catalytically active nanomaterials: a promising candidate for artificial enzymes. Acc Chem Res 47:1097–1105
16. Jiang B, Duan DM, Gao LZ, Zhou MJ, Fan KL, Tang Y, Xi JQ, Bi YH, Tong Z, Gao GF, Xie N, Tango A, Nie GH, Liang MM, Yan XY (2018) Standardized assays for determining the catalytic activity and kinetics of peroxidase-like nanozymes. Nat Protoc 13:1506–1520

17. Wei H, Wang EK (2013) Nanomaterials with enzyme-like characteristics (nanozymes): next-generation artificial enzymes. Chem Soc Rev 42:6060–6093
18. Wu JX, Wang XY, Wang Q, Lou ZP, Li SR, Zhu YY, Qin L, Wei H (2019) Nanomaterials with enzyme-like characteristics (nanozymes): next-generation artificial enzymes (II). Chem Soc Rev 48:1004–1076
19. Song YJ, Qu KG, Zhao C, Ren JS, Qu XG (2010) Graphene oxide: intrinsic peroxidase catalytic activity and its application to glucose detection. Adv Mater 22:2206–2210
20. Peng J, Weng J (2017) Enhanced peroxidase-like activity of MoS_2/graphene oxide hybrid with light irradiation for glucose detection. Biosens Bioelectron 89:652–658
21. Kim K, Chaudhari KN, Kim S, Kim Y, Shin KS (2021) Facile single-step synthesis of CurGO nanocomposite through simultaneous reduction process and its peroxidase mimic activity. Indus Engin Chem 95:388–396
22. Wang CG, Liu YP, Lan L, Tan HF (2013) Graphene wrinkling: formation, evolution and collapse. Nanoscale 5:4454
23. Vilian ATE, Dinesh B, Rethinasabapathy M, Hwang S, Jin C, Huh YS, Han Y (2018) Hexagonal Co_3O_4 anchored reduced graphene oxide sheets for high-performance supercapacitors and non-enzymatic glucose sensing. J Mater Chem A 6:14367–14379
24. Ahmed SR, Takemeura K, Li TC, Kitamoto N, Tanaka T, Suzuki T, Park EY (2017) Size-controlled preparation of peroxidase-like graphene-gold nanoparticle hybrids for the visible detection of norovirus-like particles. Biosens Bioelectron 87:558–565
25. Schoedel A, Li M, Li D, Keeffe MO, Yaghi OM (2016) Structures of metal-organic frameworks with rod secondary building units. Chem Rev 116:12466–12535
26. Wang YX, Zhao MT, Ping JF, Chen B, Cao XH, Huang Y, Tan CL, Ma QL, Wu SX, Yu YF, Lu QP, Chen JZ, Zhao W, Ying YB, Zhang H (2016) Bioinspired design of ultrathin 2D bimetallic metal-organic-framework nanosheets used as biomimetic enzymes. Adv Mater 28:4149–4155
27. Dolgopolova EA, Brandt AJ, Ejegbavwo OA, Duke AS, Maddumapatabandi TD, Galhenage RP, Larson BW, Reid OG, Ammal SC, Heyden A, Chandrashekhar M, Stavila V, Chen DA, Shustova NB (2017) Electronic properties of bimetallic metal-organic frameworks (MOFs): tailoring the density of electronic states through MOF modularity. J Am Chem Soc 139:5201–5209
28. Moran CM, Joshi JN, Marti RM, Hayes SE, Walton KS (2018) Structured growth of metal-organic framework MIL-53(Al) from solid aluminum carbide precursor. J Am Chem Soc 140:9148–9153
29. Cui JD, Ren SZ, Sun BT, Jia SR (2018) Optimization protocols and improved strategies for metal-organic frameworks for immobilizing enzymes: current development and future challenges. Coord Chem Rev 370:22–41
30. Niu XH, Shi QR, Zhu WL, Liu D, Tian HY, Fu SF, Cheng N, Li SQ, Smith JN, Du D, Lin YH (2019) Unprecedented peroxidase-mimicking activity of singleatom nanozyme with atomically dispersed Fe-Nx moieties hosted by MOF derived porous carbon. Biosens Bioelectron 142:1–8
31. Liu Z, Wang F, Ren R, Qu X (2019) A series of MOF/Ce-based nanozymes with dual enzyme-like activity disrupting biofilms and hindering recolonization of bacteria. Biomaterials 208:21–31
32. Qiao YX, Liu Q, Lu SY, Chen G, Gao SY, Lu WB, Sun XP (2020) High-performance non-enzymatic glucose detection: using conductive Ni-MOF as an electrocatalyst. J Mater Chem B 8:5411–5415
33. Hu ZF, Yin YH, Liu QY, Zheng XW (2019) A functional FePt@MOFs (MIL-101(Fe)) nanoplatform for high efficient colorimetric determination of H_2O_2. Analyst 144:2716
34. Dang XM, Zhao HM (2020) Bimetallic Fe/Mn metal-organic-frameworks and Au nanoparticles anchored carbon nanotubes as a peroxidase-like detection platform with increased active sites and enhanced electron transfer. Talanta 210:120678
35. Li Y, Zhao XR, Li P, Huang YF, Wang J, Zhang JM (2015) Highly sensitive Fe_3O_4 nanobeads/graphene-based molecularly imprinted electrochemical sensor for 17β-estradiol in water. Anal Chim Acta 884:106–113
36. Li Y, Xu WK, Zhao XR, Huang YF, Kang JJ, Qi Q, Zhong CL (2018) Electrochemical sensors based on molecularly imprinted polymer on Fe_3O_4/graphene modified by gold nanoparticles for highly selective and sensitive detection of trace ractopamine in water. Analyst 143:5094–5102
37. Cheng T, Li X, Huang P, Wang H, Wang MX, Yang WM (2019) Colorimetric and electrochemical (dual) thrombin assay based on the use of a platinum nanoparticle modified metal-organic framework (type Fe-MIL-88) acting as a peroxidase mimic. Microchim Acta 186:94
38. Wang J, Liu C, Li JS, Luo R, Hu XR, Sun XY, Shen JY, Han WQ, Wang LJ (2017) In-situ incorporation of iron-copper bimetallic particles in electrospun carbon nanofibers as an efficient Fenton catalyst. Appl Catal B Environ 207:316–325
39. Zhang Y, Zhou ZF, Wen FF, Tan J, Peng T, Lou BQ, Wang HG, Yin SX (2018) A flower-like MoS_2-decorated $MgFe_2O_4$ nanocomposite: mimicking peroxidase and colorimetric detection of H_2O_2 and glucose. Sens Actuators B Chem 275:155–162
40. Wang JN, Wei TX, Liu YC, Bao MY, Feng R, Qian YX, Yang X, Si L, Dai ZH (2020) Colloidal-sized zirconium porphyrin metal-organic frameworks with improved peroxidase-mimicking catalytic activity, stability and dispersity. Analyst 145:3002
41. Chen JJ, Gao HJ, Li ZH, Li YX, Yuan Q (2020) Ferriporphyrin-inspired MOFs as an artificial metalloenzyme for highly sensitive detection of H_2O_2 and glucose. Chin Chem Lett 31:1398–1401
42. Ngo YLT, Nguyen PL, Choi WM, Chung JS, Hur SH (2020) Highly sensitive smartphone-integrated colorimetric glucose sensor based on $MnFe_2O_4$-graphitic carbon nitride hybrid nanostructure. Mater Res Bull 129:110910
43. Yuan K, Song TQ, Wang DW, Zou Y, Li JF, Zhang XT, Tang ZY, Hu WP (2018) Bimetal-organic frameworks for functionality optimization: MnFe-MOF-74 as a stable and efficient catalyst for the epoxidation of alkenes with H_2O_2. Nanoscale 10:1591–1597
44. Fan XT, Tian RZ, Wang TT, Liu SD, Wang L, Xu JY, Liu JQ, Ma M, Wu ZZ (2018) An ultrathin iron-porphyrin based nanocapsule with high peroxidase-like activity for highly sensitive glucose detection. Nanoscale 10:22155–22160
45. Wu N, Wang YT, Wang XY, Guo FN, Wen H, Yang T, Wang JH (2019) Enhanced peroxidase-like activity of AuNPs loaded graphitic carbon nitride nanosheets for colorimetric biosensing. Anal Chim Acta 1091:69–75
46. Liu YL, Zhao XJ, Yang XX, Li YF (2013) A nanosized metal-organic framework of Fe-MIL-88NH_2 as a novel peroxidase mimic used for colorimetric detection of glucose. Analyst 138:4526–4531
47. Su L, Qin WJ, Zhang HG, Rahman ZU, Ren CL, Ma SD, Chen XG (2015) The peroxidase/catalase-like activities of MFe_2O_4 (M=Mg, Ni, Cu) MNPs and their application in colorimetric biosensing of glucose. Biosens Bioelectron 63:384–391
48. Wang QQ, Zhang XP, Huang L, Zhang ZQ, Dong SJ (2017) One-pot synthesis of Fe_3O_4 nanoparticle-loaded 3D porous graphene nanocomposites with enhanced nanozyme activity for glucose detection. ACS Appl Mater Interfaces 9:7465–7471
49. Ai LH, Li LL, Zhang CH, Fu J, Jiang J (2013) MIL-53(Fe): a metal-organic framework with intrinsic peroxidase-like catalytic activity for colorimetric biosensing. Chem Eur J 19:15105–15108
50. Qin FX, Jia SY, Wang FF, Wu SH, Song J, Liu Y (2013) Hemin@metal–organic framework with peroxidase-like activity and its application to glucose detection. Catal Sci Technol 3:2761–2768
51. Bandi R, Alle M, Park CW, Han SY, Kwon GJ, Kim NH, Kim JC, Lee SH (2021) Cellulose nanofibrils/carbon dots composite nanopapers for the smartphone-based colorimetric detection of hydrogen peroxide and glucose. Sens Actuators B Chem 330:129330

52. Ngo YLT, Nguyen PL, Jana J, Choi WM, Chung JS, Hur SH (2021) Simple paper-based colorimetric and fluorescent glucose sensor using N-doped carbon dots and metal oxide hybrid structures. Anal Chim Acta 1147:187–198